

## Development of a special heat structure model for the core makeup tank and its assessment using the SPACE code

Min Gi Kim<sup>a</sup>, Jae Jun Jeong<sup>\*a</sup>, Jong-Hyuk Lee<sup>b</sup>, Kyungdoo Kim<sup>b</sup>, Hyun-Sik Park<sup>c</sup>

<sup>a</sup>School of Mechanical Engineering, Pusan National University (PNU)

<sup>b</sup>Virtual Nuclear Power Plant Technology Development Division, Korea Atomic Energy Research Institute (KAERI)

<sup>c</sup>Innovative System Safety Research Division, Korea Atomic Energy Research Institute (KAERI)

\*Corresponding author: jjjeong@pusan.ac.kr

### 1. Introduction

The SMART [1], a Korean small modular reactor, has various passive safety systems. For example, a passive safety injection system (PSIS) of SMART includes four core makeup tanks (CMTs) and four safety injection tanks (SITs) for providing core cooling. Recently, some integral effect tests [2] were performed using the integral effect test facility, SMART-ITL [3], to assess the PSIS performance. Also, as a part of the model development and validation for the thermal-hydraulic safety analysis code, SPACE [4], we simulated the PSIS performance tests, F101 and F102. It was found that the SPACE code did not accurately calculate the PSIS's performance. It is because the SPACE code uses the bulk liquid temperature to calculate the interfacial heat transfer between water and interface, so the overall interfacial heat transfer was over-predicted. In our previous work [5], we developed a special thermal-hydraulic model for CMT which can realistically calculate the interfacial heat transfer. However, since the special thermal-hydraulic model for CMT considers the tank as one control volume, the heat structure model that can reasonably consider the heat transfer between the inner tank wall and the steam was needed. In this paper, we developed a special heat structure model for the wall heat transfer of CMT. Then, a special heat structure model was assessed using the SPACE code. The results shows that the special heat structure model for CMT predicts the behavior of CMT and SIT reasonably well. Future improvements have been specified.

### 2. Development and assessment of the special heat structure model for the CMT

#### 2.1 Development of the special heat structure model

Each tank is at first filled with subcooled water, and the temperature of the tank wall is equal to the temperature of the subcooled water in the tank before the CMT/SIT operation. When the safety injection begins, the tank is gradually filled with hot steam from the top. As condensation occurs on the inner wall of the tank, the heat transfer from the steam to the wall is important. Because the heat transfer between the subcooled water and the wall is nearly negligible, it is not considered in the special heat structure model.

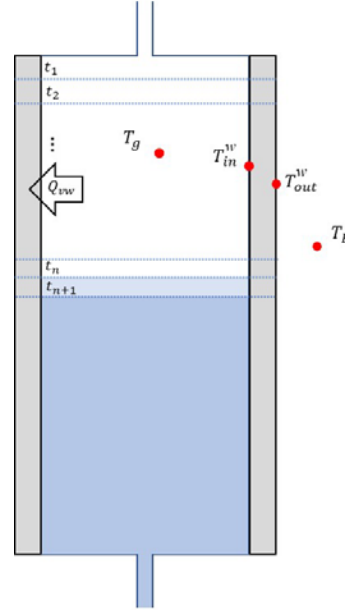


Fig. 1. Simplified CMT temperature distribution.

Fig. 1. shows the simplified temperature distribution of the CMT. Assuming the steam reaches the top of the tank at  $t=0$  and the vertically stratified water level decreases each time step. Then, it can be considered that a thin slice of the tank wall is exposed to the steam phase each time step. In this point of view, the steam-exposed metal wall can be axially split into  $n$  slices of heat structure. If we assume that axial heat conduction in the wall is negligible, the energy equation for the  $i$ -th slice of the wall is followed as:

$$\begin{aligned} & \delta\alpha_i M_{\text{tank}} C_p \frac{d\bar{T}_i^w}{dt} \\ & = \delta\alpha_i h_{in} A_{in} (T_g - T_{in,i}^w) - \delta\alpha_i h_{out} A_{out} (T_{out,i}^w - T_B) \end{aligned} \quad (1)$$

By neglecting the thermal resistance to the thermal conductivity of the wall,  $T_{in,i}^w = T_{out,i}^w = \bar{T}_i^w$  is assumed. Instead, the convective heat transfer coefficient of the outer wall is adjusted to compensate for this error as follows:

$$\frac{1}{h_{out}^{\text{mod}}} = \frac{1}{h_{out}} + \frac{1}{k / \delta x} \quad (2)$$

Then, Eq. (1) is represented as:

$$\begin{aligned} M_{\text{tank}} C_p \frac{d\bar{T}_i^w}{dt} &= h_{in} A_{in} (T_g - \bar{T}_i^w) - h_{out}^{\text{mod}} A_{out} (\bar{T}_i^w - T_B) \\ &= -(h_{in} A_{in} + h_{out}^{\text{mod}} A_{out}) \bar{T}_i^w + h_{in} A_{in} T_g + h_{out}^{\text{mod}} A_{out} T_B. \end{aligned} \quad (3)$$

Assuming all the parameters in Eq. (3) except  $\bar{T}_i^w$  remain constant during a time step advance, the solution for the  $i$ -th element of the heat structure is:

$$\bar{T}_i^w(t) = \begin{cases} T_{\text{initial}}^w e^{-\lambda(t-t_i)} + T_{\infty}^w [1 - e^{-\lambda(t-t_i)}] & \text{for } t > t_i, \\ T_{\text{initial}}^w & \text{for } t \leq t_i, \end{cases} \quad (4)$$

$$\text{where } \lambda = \frac{h_{in} A_{in} + h_{out}^{\text{mod}} A_{out}}{M_{\text{tank}} C_p}, \quad T_{\infty}^w = \frac{h_{in} A_{in} T_g + h_{out}^{\text{mod}} A_{out} T_B}{h_{in} A_{in} + h_{out}^{\text{mod}} A_{out}}$$

and  $T_{\text{initial}}^w$  is the initial inner wall temperature.

Then, the total convective heat transfer from the steam to the inner wall surface at  $t_n$  can be calculated as:

$$\begin{aligned} Q_{vw}(t_n) &= \sum_{i=1}^n \delta\alpha_i h_{in} A_{in} [T_g(t_n) - \bar{T}_i^w(t_n - t_i)] \\ &= \alpha_n h_{in} A_{in} \left[ T_g(t_n) - \frac{1}{\alpha_n} \sum_{i=1}^n \delta\alpha_i \bar{T}_i^w(t_n - t_i) \right]. \end{aligned} \quad (5)$$

If we use Eq. (5), we need to keep track of the void fractions at all time steps as well as the average wall temperatures of all heat structure slices. This necessitates a large amount of memory and inconvenient calculations.

Assuming that the average wall temperature at time  $t_n$  is  $\bar{T}^w(t_n)$ . It can be written as:

$$\alpha_n \bar{T}^w(t_n) = \sum_{i=1}^n \delta\alpha_i \bar{T}_i^w(t_n - t_i). \quad (6)$$

Then, Eq. (5) can be rewritten as:

$$Q_{vw}(t_n) = \alpha_n h_{in} A_{in} [T_g(t_n) - \bar{T}^w(t_n)]. \quad (7)$$

A recursive formulation is constructed from Eq. (6) to conveniently calculate  $\bar{T}^w(t_{n+1})$ :

$$\begin{aligned} \alpha_{n+1} \bar{T}^w(t_{n+1}) &= \sum_{i=1}^{n+1} \delta\alpha_i \bar{T}_i^w(t_{n+1} - t_i) \\ &= \sum_{i=1}^n \delta\alpha_i \bar{T}_i^w(t_{n+1} - t_i) + \delta\alpha_{n+1} T_{\text{initial}}^w \end{aligned}$$

$$\begin{aligned} &= \sum_{i=1}^n \delta\alpha_i \left[ \bar{T}_i^w(t_n - t_i) + \frac{d\bar{T}_i^w}{dt} \Big|_{t_n - t_i} \delta t_{n+1} \right] + \delta\alpha_{n+1} T_{\text{initial}}^w \\ &= \alpha_n \bar{T}^w(t_n) + \sum_{i=1}^n \delta\alpha_i \frac{d\bar{T}_i^w}{dt} \Big|_{t_n - t_i} \delta t_{n+1} + \delta\alpha_{n+1} T_{\text{initial}}^w \end{aligned} \quad (8)$$

where  $\delta t_{n+1} = t_{n+1} - t_n$ . The right-hand side of Eq. (8)'s derivative term can be approximated as:

$$\begin{aligned} &\sum_{i=1}^n \delta\alpha_i \frac{d\bar{T}_i^w}{dt} \Big|_{t_n - t_i} \\ &\approx \sum_{i=1}^n \delta\alpha_i \left[ -\lambda \bar{T}_i^w(t_n - t_i) + \lambda T_{\infty}^w + \frac{dT_{\infty}^w}{dt} (1 - e^{-\lambda(t_n - t_i)}) \right] \\ &= \sum_{i=1}^n \delta\alpha_i \left[ -\lambda \bar{T}_i^w(t_n - t_i) + \lambda T_{\infty}^w + \frac{dT_{\infty}^w}{dt} \right] \\ &= -\lambda \sum_{i=1}^n \delta\alpha_i \bar{T}_i^w(t_n - t_i) + \alpha_n \left[ \lambda T_{\infty}^w + \frac{dT_{\infty}^w}{dt} \right] \\ &= -\lambda \alpha_n \bar{T}^w(t_n) + \alpha_n \left[ \lambda T_{\infty}^w + \frac{dT_{\infty}^w}{dt} \right] \end{aligned} \quad (9)$$

Because  $\lambda$  is expected large enough,  $e^{-\lambda(t_n - t_i)}$  in Eq. (8) converges to 0 rapidly. By replacing the derivative term in Eq. (8) with Eq. (9), the relation between  $\bar{T}^w(t_n)$  and  $\bar{T}^w(t_{n+1})$  can be written as:

$$\begin{aligned} \alpha_{n+1} \bar{T}^w(t_{n+1}) &= (1 - \lambda \delta t_{n+1}) \alpha_n \bar{T}^w(t_n) \\ &\quad + \alpha_n \left[ \lambda T_{\infty}^w + \frac{dT_{\infty}^w}{dt} \right] \delta t_{n+1} + \delta\alpha_{n+1} T_{\text{initial}}^w \end{aligned} \quad (10)$$

By using Eq. (10), it is possible to use Eq. (7) to calculate the convective heat transfer between the steam and the inner wall.

## 2.2 Assessment of the special heat structure model

We implemented the special heat structure model into the SPACE code and simulated the SMART-ITL PSIS performance tests, F101 and F102, [6]. The detailed information and test scenario are described in the previous study [5]. In this paper, we compared the simulations with/without the special heat structure model to the experimental data. Both cases used the special thermal-hydraulic model for the CMT [5].

Using the special heat structure model, the heat loss at the tank wall is taken into account. The outside wall heat transfer coefficient and the surrounding temperature were considered as the boundary conditions.

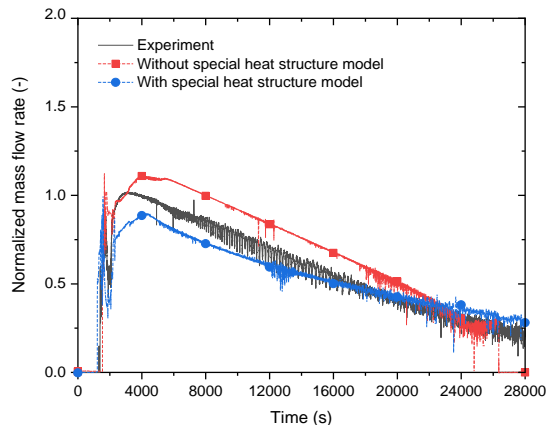


Fig. 2. Measured vs. calculated CMT #1 injection flow rate (F101 test).

For the F101 test, the measured and predicted CMT injection flow rates are shown in Fig. 2. Because both simulations used a special thermal-hydraulic model, the interfacial heat transfer in the tank was realistically calculated and the safety injection was performed well. However, in the case without the special heat structure model, heat transfer through the tank wall was not considered, so the injection flow of the CMT outlet was over-predicted compared to the experiment. With the special heat structure model, the injection flow rate of the CMT is under-predicted compared to the experiment and the CMT empties more slowly due to the steam condensation on the wall. Also, the overall behavior was predicted close to the experiment than without the special heat structure model case. This indicates that the special heat structure model should be considered to realistically predict the behavior of the CMT.

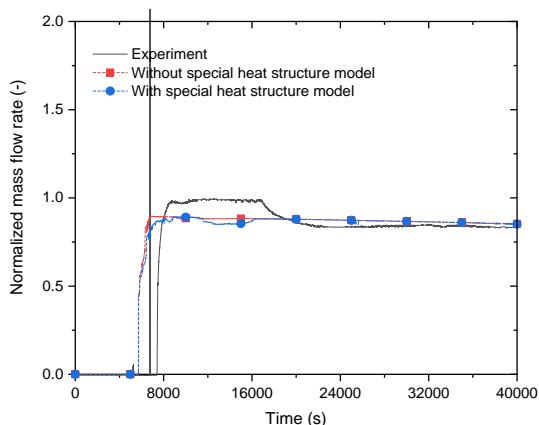


Fig. 3. Measured vs. calculated SIT #1 injection flow rate (F102 test).

We also simulated the F102 test to confirm the injection flow prediction performance of the SIT. Fig. 3 shows the measured and predicted SIT injection flow rates in the F102 test. In this simulation, there was little difference between the with/without special heat structure model cases. This is because the temperature difference between the inner wall and the steam at the

time of the SIT operation is smaller than the time of the CMT operation (F101 test), and the injection flow rate through the SIT is relatively small compared to the CMT. Therefore, heat transfer through the wall was negligible compared to the simulation of the F101 test.

In conclusion, the special heat structure model reasonably considered the heat transfer between the inner wall and steam in the CMT and SIT. Also, the result of simulations indicated that it is necessary to use a special heat structure model to realistically predict the behaviors of the CMT and SIT. However, more assessments under various conditions are still needed.

### 3. Conclusions

In this paper, we developed a special heat structure model for CMT and SIT to realistically consider the wall heat transfer when the special thermal-hydraulic model for CMT is used. By assuming a vertically stratified flow is formed in the CMT, we established a realistic heat transfer equation and developed it as a model. The special heat structure model was then implemented into the SPACE code and assessed using the SMART-ITL PSIS performance tests. When the special heat structure model was used, the wall heat transfer of CMT and SIT was realistically calculated, and the modified SPACE code predicted the behavior of the PSIS reasonably. However, it is necessary to be assessed more under various test or operation conditions.

### ACKNOWLEDGEMENT

This research was supported by KAERI and King Abdullah City for Atomic and Renewable Energy (K.A.CARE), Kingdom of Saudi Arabia, within the Joint Research and Development Center.

### REFERENCES

- [1] K.K. Kim, W.J. Lee, S. Choi, H.R. Kim, and J.J. Ha, SMART: the first licensed advanced integral reactor, *Journal of Power and Energy Engineering*, 8, pp. 94– 102, 2014
- [2] H.S. Park, H. Bae, S.U. Ryu, B.G. Jeon, J.H. Yang, Y.S. Kim, E.K. Yun, J.M. Kim, N.H. Choi, Y.C. Shin, K.H. Min, Y.G. Bang, M.J. Kim, C.J. Seo, and S.J. Yi, Core Cooling Behaviors in SMART-ITL with Passive Safety Injection System and Passive Residual Heat Removal System during a SBLOCA Scenario, *Transactions of the Korean Nuclear Society Autumn Meeting*, Gyeongju, Korea, May 18-19, 2017.
- [3] H. S. Park, S. J. Yi, C. H. Song, SMR accident simulation in experimental test loop, *Nuclear Engineering International*, Nov. (2013) pp.12–15.
- [4] S. J. Ha, C. E. Park, K. D. Kim, and C. H. BAN, Development of the SPACE code for nuclear power plants, *Journal of Nuclear engineering and technology*, 43(1), pp. 45-62, 2011.
- [5] M.G. Kim, J. J. Jeong, J. H. Lee, K. D. Kim, and H. S. Park, Development of the lumped parameter core makeup tank model of SMART and assessment using the SPACE code, *Transactions of Korean Nuclear Society Spring Meeting*, Korea, 2021.

[6] H. Bae, S.U. Ryu, J.Y. Kang, J.H. Yang, Y.S. Kim, and H.S. Park, Data Analysis Report: 4-Train PSS tests, S-750-NV457-005, KAERI.

### NOMENCLATURE

$\alpha$  : Void fraction  
 $\delta\alpha_i$  :  $\alpha(t_i) - \alpha(t_{i-1})$   
 $A_{in}$  : Inner side wall area  
 $A_{out}$  : Outer side wall area  
 $C_p$  : Specific heat of the tank wall  
 $h_{in}$  : Inner side heat transfer coefficient  
 $h_{out}$  : Outer side heat transfer coefficient  
 $h_{out}^{mod}$  : Modified outer side heat transfer coefficient  
 $k$  : The wall conductivity  
 $M_{tank}$  : Total mass of the cylindrical part of the tank  
 $Q_{vw}$  : The heat transfer from the steam to the inner wall  
 $T^s$  : The saturation temperature  
 $T_{initial}^w$  : The initial inner wall temperature  
 $T_{in}^w$  : Inner side wall temperature  
 $T_{out}^w$  : Outer side wall temperature  
 $T_g$  : Vapor temperature  
 $T_B$  : Bulk temperature  
 $\bar{T}^w$  : The average wall temperature  
 $\delta x$  : The thickness of the tank wall  
 $t$  : Time